TWENTYFIFTH EUROPEAN ROTORCRAFT FORUM

Paper n° C1

ENGINE-AIRFRAME INTEGRATION USING NAVIER-STOKES SIMULATION OF TWO AGUSTA HELICOPTERS UPPER DECK COWL AND AIR INDUCTION SYSTEM

BY

M. Loka, P. Tran, M. Moore, M. Robichaud and W. Di Bartolomeo
Pratt & Whitney Canada,
1000 Marie-Victorin,
Longueuil, Québec,
CANADA, J4G 1A1

L. Medici and A. Saporiti
Agusta SpA,
Viale Agusta 520,
21017 Cascina Costa di Samarate (VA),
ITALY

September 14-16, 1999
ROME
ITALY

ASSOCIAZIONE INDUSTRIE PER L'AEROSPAZIO, I SISTEMI E LA DIFESA
ASSOCIAZIONE ITALIANA DI AERONAUTICA ED ASTRONAUTICA

1. ABSTRACT

At Pratt & Whitney Canada, computational fluid dynamics (CFD) is used to optimize component or system designs from performance, cost, weight and operability perspectives. Driven by shorter engine development cycles, the lead-time for the components and systems studied is also shortened. As such, the use of CFD has been adopted as a potential competitive advantage in providing the opportunity to engineer these components and systems to meet their targets, both from the performance and schedule aspects. In this context, the role of CFD is to allow quick design assessments, so that the aerodynamicist can evaluate numerous and innovative concepts and make engineering decisions to achieve the final design. In addition, the methodology provides a means to evaluate performance penalties related to engine installation on specific aircraft due to additional pressure losses, inlet distortion and exhaust backpressure. As such, it yields both qualitative and quantitative assessments of the flow phenomena associated with the integration of the engine in the airframe. CFD can be used to provide guidelines to the airframe manufacturer in order to improve designs or incorporate geometrical features to reduce such effects. The present methodology was used to design P&WC hardware such as the PW150 front inlet case or turboshaft swept exhaust ducts and stubs. However, the project as described in this paper represents the first attempt at analysing simultaneously external and internal flows.

2. INTRODUCTION

This paper presents CFD simulations used in the integration of the gas turbine engine on a helicopter. At Pratt & Whitney Canada, flow simulation is used in the conceptual design phase to determine the optimal engine-airframe match over the flight envelope. In collaboration with the airframe manufacturer, the goal becomes to develop the most appropriate aircraft loft lines at an early stage. Two Agusta helicopters are highlighted: the AB139 helicopter powered by two PT6C-67C engines and the A119 Koala powered by a single PT6B-37 engine.

The Agusta 119 Koala is an eight-seater light single turbine helicopter designed for passenger transport and aerial works, see Fig. 1. The air induction system of the rotorcraft consists of three screened openings in the upper cowl leading to the engine plenum. Air is sucked into the compressor through a radial intake case equipped with 6 struts as shown in Fig. 3.

The Agusta AB139 helicopter is powered by two engines seated in separate compartments on the port and starboard sides of the upper deck. The inlet system is of the sideways-facing type as shown in Fig. 9. Front and rear inlet lips are located just below the aircraft screen to better guide the flow into the compartment. The engines are equipped with inward-flowing radial intake passages containing 6 struts.

The complete viscous analysis of the external flow field around the upper deck of the helicopter and internal flow field in the engine compartment was undertaken to evaluate various airframe cowl/inlet system configurations. The study includes all components of its air induction system such as compartment inlet lip, aircraft screen, engine plenum, engine intake screen, and engine intake case including the intake struts as shown in Fig. 9.

Hover and cruise were the two flight conditions of primary interest for the current helicopters. Due to their external flowfield differences, two different computing domains were required. A preliminary Euler solution is obtained on a coarse unstructured mesh then mapped onto the fine structured mesh, providing an adequate initial solution and thereby reducing computing time. Boundary condition imposition was challenging due to the novelty of the problem.

The analysis provided a good understanding of the loss mechanisms with their respective contributions to the overall pressure loss and allowed a qualitative assessment of configuration changes for possible loss reductions. Configuration changes achieved performance improvements by reducing the inlet losses as well as providing more uniform flow distribution at the compressor face. Previously, the loss

assessment of such air induction systems was based on empirical 1-D pressure loss models coupled with representative descriptions for the external flow field such as pressure distribution along the aircraft surface. CFD has made it possible to study the flow phenomena around a helicopter in a virtual wind tunnel environment. To conduct such an evaluation in a wind tunnel would require considerable time and investment.

3. FLOW SOLVER

The flow calculations were conducted using NS3D, a P&WC developed finite element, compressible, turbulent flow solver [1,2]. NS3D is the result of collaboration between P&WC and the CFDLab research group at Concordia University. A pressure dissipation term is introduced into the continuity equation to avoid the odd-even decoupling, thus permitting the use of equal order interpolation for velocities and pressure. The momentum equations are stabilised using the Streamline Upwind Petrov-Galerkin scheme. The flow turbulence is taken into account by the two-equation k-ω model. The flow solver can accommodate multi-block, structured grids or unstructured grids composed of tetrahedral/prism elements as shown in Fig. 2.

4. GRID GENERATION

A commercial package, ICEM-CFD, is used for grid generation. The package includes ICEM-Hexa, a hexahedral multi-block structured mesh generator and ICEM-Tetra, an octree-based tetrahedral mesh generator. Both grid generation tools are used in the current CFD analysis methodology for complex geometries at Pratt & Whitney Canada.

5. IMPOSITION OF BOUNDARY CONDITIONS

5.1 HOVER CONDITION

As shown in Fig. 10, the external boundary was built as a flat cylinder where a symmetry BC is imposed along the side. The upper boundary is an inlet where a radial profile of circumferential and downward velocities is imposed. The lower boundary is modelled as a static pressure imposed exit. The upper cowl, plenum and intake case surfaces are specified as walls. It is of interest to determine the aerodynamic profile at the compressor face from effects of the geometry upstream. To eliminate any prejudice from boundary condition imposition, a constant area extension was added downstream of the compressor face. A static pressure imposition at the extension exit ensures the correct engine mass flow and no disturbances to the flow upstream up to the compressor face.

5.2 FORWARD FLIGHT CONDITION

As shown in Fig. 11, the external boundary for the forward flight condition was changed from a cylinder to a box. The upstream boundary is a mass flow imposed inlet calculated from the domain inlet area and helicopter forward speed. The downstream boundary is a static pressure imposed exit. Upper, lower and side boundaries are modelled as symmetry surfaces. A static rotor mast was also added to the analysis to assess the effect of the rotor wake flow into the plenum. Rotor downwash is not modelled in forward flight. VSAERO assessments computed at Agusta showed that the rotor downwash interacts with the airframe downstream of the engine compartment openings.

6. ANALYSIS OF LOSS MECHANISMS

In order to minimize engine-airframe integration losses, the external and internal flow fields in potential loss regions have to be assessed. The inlet system pressure losses stem from the level of ram recovery, aircraft screen losses, sudden expansion, plenum losses and intake screen losses.

6.1 RAM RECOVERY

The level of ram recovery described by the dynamic pressure recovery coefficient C_p changes locally at different curvatures of the aircraft loft lines. The aircraft screen and sudden expansion losses are dependent on the local C_p. Local C_p levels vary from each side of the aircraft screens as well as differ between the top and the flanks of the aircraft (Fig. 12).

6.2 SUDDEN EXPANSION

In forward flight, the width of the streamtube entering the engine compartment in a sideways-facing inlet system is related to the local curvature of aircraft lines or the level of pressure recovery. The width of the streamtube also dictates the local flow velocity at the aircraft screen. Lower velocity result in lower screen losses. The streamtube then expands and fills the engine plenum resulting in a sudden expansion loss. In hover, the current loss mechanism becomes a minor contributor to the overall loss level (Fig. 13).

6.3 PLENUM LOSS

In hover, the rotor downwash creates a pressure gradient similar to that of the pressure recovery coefficient C_p. This leads to a non-uniformity of the flow inside the engine compartment, or plenum. This may result in a negative effect on the engine performance but may not induce pressure losses as such. Examples of Mach number distributions and streamlines entering the engine plenum are shown for the Koala in hover and forward flight in Figs. 4, 5 and 6.

6.4 SCREEN LOSSES

Aircraft and engine intake screens provide passive protection for icing and Foreign Object Damage (FOD). They inherently address the certification requirements for the aircraft powerplant. Their loss contribution is minor compared to the other loss factors.

The mechanism of screen losses is observed to come from flow acceleration through the screen mesh forming jets of relatively high velocity behind the openings and wakes of relatively low velocity behind the cylindrical wires. The high momentum flow of the jets reenergize the low momentum flow of the wakes generating a mixing process thereby creating a uniform flow downstream. The largest contribution to the total pressure loss through the screen comes from the mixing process itself.

Total pressure losses across the screen are based on the non-dimensional loss coefficient λ:

$$\lambda = \frac{\Delta P_T}{q_{upstream}}$$

This relation assumes a flow normal to the screen. Flow incidence is taken into account by using the normal component to the screen. The screen blockage, or solidity, is defined as the ratio of blocked area over total screen area. In the current investigation, two sets of screens were studied: the aircraft screen composed of a coarse wire-mesh and the engine intake screen with a higher solidity (approximately twice the aircraft screen solidity). Screen pressure losses are obtained from curves relating inlet Mach number, screen solidity and loss coefficient λ taken from Cornell [3].

7. PRESSURE LOSS OPTIMIZATION

The analysis of CFD results leads to qualitative assessment of the pressure losses and therefore means of loss reduction are determined. The largest contribution is observed to come from the sudden expansion, or dump, into the engine compartment. It is related to the ram recovery. Various AB139/PT6C-67C loft configurations were considered to assess the impact on this loss mechanism, see Figs. 14 to 17. Figure 18 shows the increase in streamtube width through geometry modifications. The pressure loss results are summarised in Table 1.

CRUISE 155 KTAS Loss Contribution	Geom. 1 $\frac{\Delta P}{P}$ %	Geom. 2 $\frac{\Delta P}{P}$ %	Geom. 3 $\frac{\Delta P}{P}$ %	Geom. 4 $\frac{\Delta P}{P}$ %
Aircraft Inlet	Baseline	-0.20	-0.70	-0.87
Overall	Baseline	+0.04	-1.06	-1.03

Streamlining is a common solution for reducing flow separation in a sudden expansion type of configuration. The inlet lip of the AB139 at the upstream side was elongated and shaped to conform to the streamtube path entering the plenum, creating a much more pronounced inlet lip at the engine fore-cowling surface as shown in Fig. 19. The intent was to better guide the flow into the engine compartment and maintain it attached for a longer distance. This was targeted to reduce the dump losses. Some pressure loss reduction was achieved at the inlet to the engine compartment as a consequence of the inlet lip better guiding the flow. However, the improvement is negated by an increase in pressure losses within the engine inward-flowing radial intake case and intake struts. As a result, the overall inlet system does not improve or deteriorate due to the modification of the inlet lip. The inlet lip modification therefore, was not considered as a viable option due to the additional weight, complexity of the design, and no performance improvement to the overall inlet system.

A flow divider, or baffle, was added to the A119 Koala configuration to assess potential benefits to overall flow distribution in the inlet system. The flow divider can improve the flow uniformity by dividing the space into dedicated passages feeding particular parts of the intake (Fig. 7). The analysis shows that the pressure losses in the air induction system have increased with the addition of the flow divider. Its effects on the aerodynamic performance of the air induction system were completed in forward flight. Fig. 8 shows the Mach number distribution in the plenum. It is observed that the addition of the baffle induces high incidence on the 4 and 8 o'clock struts therefore increasing pressure losses. To further improve the flow divider, it was moved forward 1" to force more flow to the bottom half of the intake case. The pressure losses did not change but the flow became more uniform.

8. COMPARISON WITH ANALYTICAL PERFORMANCE MODEL

The pressure losses calculated from freestream to engine screen were compared against an analytical installed performance model (Fig. 20). The analysis is based on 1-D pressure loss models coupled with representative descriptions for the external flow field such as pressure distribution along the aircraft surface. For both cruise and hover, the analytical model estimate was found to be within 10% of the CFD analysis after correction for the C_p in the region of the aircraft screens. In both hover and cruise conditions, the loss assessment using NS3D compares well with preliminary calculations using a proven P&WC methodology. The analytical installed performance model has been validated extensively on previous rotorcraft installations using flight test data.

9. CONCLUSIONS

Assessing such complex systems as the current installed engine in flight using Navier-Stokes CFD computations have proven to be beneficial. In addition to providing insight into the loss mechanisms and their respective contributions, CFD has led to a quantitative assessment of configuration changes thereby achieving performance improvements by reducing both pressure losses and improving flow uniformity.

Resolving all initial solution and BC problems on a coarse Euler grid instead of using the final very fine structured mesh is very time-efficient and should be done for complex problems such as the helicopter upper cowl and engine plenum. In this case, once the initial inviscid flow was solved, the viscous turbulent solution was obtained quickly from the Euler solution as the initial guess.

The analysis lead to a good qualitative understanding of the pressure loss mechanisms and their individual contributions. This paved the way for targeting key changes to the geometry to improve performance.

High C_p levels along the aircraft lines benefit the inlet system. The location of the air inlet opening on the aircraft determines static pressure levels and consequently C_p to which the inlet is exposed. It is not always possible to choose the most desirable location on the helicopter. However, changes in the local loft lines upstream and downstream of the engine plenum can change the C_p level.

10. FUTURE WORK

Structured grid generation for such complex geometries as the rotorcraft air induction system and upper deck cowling invariably introduces grid-dependent errors in the flow solution. These result from skewness or non-orthogonality in the grid or from regions where the mesh fineness is insufficient to capture flow features such as wakes and boundary layers. Numerical errors can also stem from the turbulence modelling.

The first source of error is being addressed by directing future work towards unstructured meshing. In addition, adaptive meshing will allow mesh optimisation and therefore minimize the required number of grid points for a given problem. The mesh adaptation includes node swapping, mesh movement, refinement and coarsening. The movement technique is based on error estimates of a numerical solution. The refinement and coarsening technique is based on gradients of aerodynamic quantities such as velocity, pressure, and density in the flow field. The mesh will also include a prism layer at the walls to ensure grid orthogonality thereby accommodating the turbulence model. Turbulence and transition modelling errors will be addressed through our CFD validation efforts based on experimental results.

It is intended to apply a screen model [4] by replacing the screen with a discontinuous interface where mass and energy are conserved, a flow direction change is applied, and a pressure loss is evaluated empirically.

Imposing constant heat flux on walls could simulate the charge heating, or pre-heating of the air before it reaches the compressor face. This would be accomplished by solving the energy equation in addition to the continuity and momentum equations. However, empirical data would be required to impose the proper wall boundary conditions.

11. REFERENCES

1. Robichaud, M.P., Di Bartolomeo, W., Heikurinen, K. and Habashi, W.G., Turboprop Air Intake Design Using 3-D Viscous Analysis, AIAA Paper 97-0171, 35th AIAA Aerospace Sciences Meeting, Reno, January 1997.

2. Tam, A., Robichaud, M.P., Tremblay, P., Habashi, W.G., Hohmeyer, M., Guevrement, G., Peeters, M.F. and Germain, P., A 3-D Adaptive Anisotropic Method for External and Internal Flows, AIAA Paper 98-0771, 36th AIAA Aerospace Sciences Meeting, Reno, January 1998.

3. Cornell, W.G., Losses in Flow Normal to Plane Screens, Transactions of the ASME, May 1958, pp. 791-799.

4. Bush, R.H., Engine Face and Screen Loss Models for CFD Application, AIAA Paper 97-2076, Proceedings of the 13th AIAA CFD Conference, Snowmass Village, Colorado, June 1997, pp. 1161-1171.

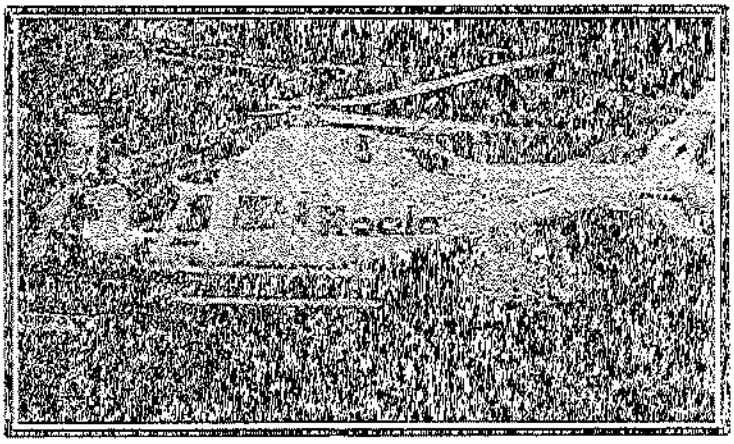

Figure 1: Picture of the Agusta 119 Koala Rotorcraft

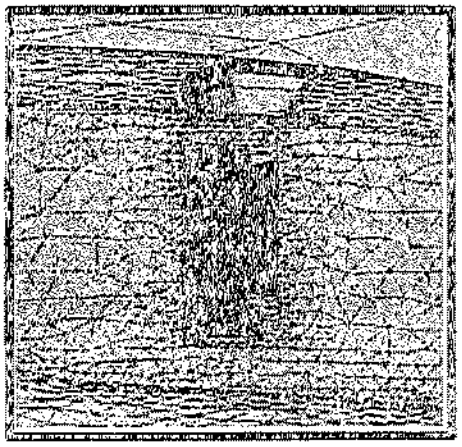

Figure 2: A119 Unstructured Tetrahedral Mesh

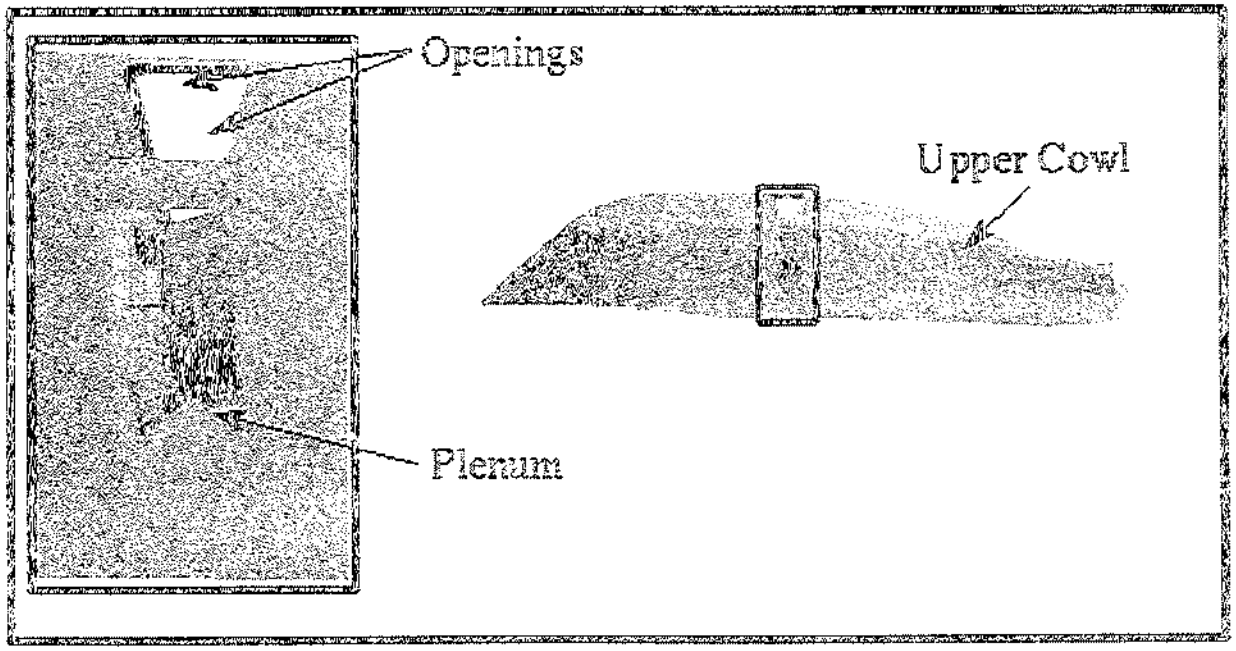

Figure 3: Geometry of the A119 Koala Air Induction System

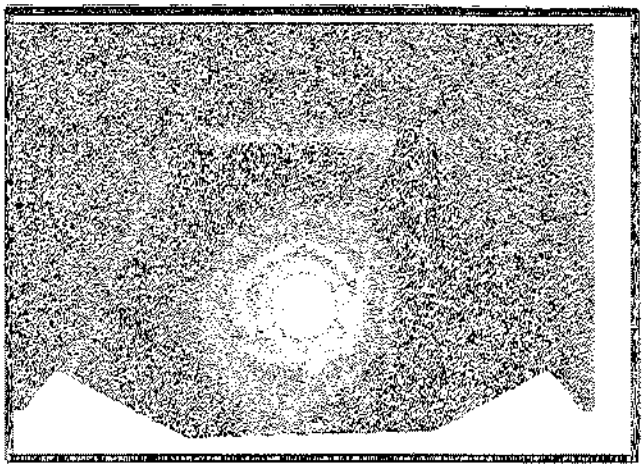

Figure 4: A119 Mach Number Distribution Inside Engine Plenum (Hover)

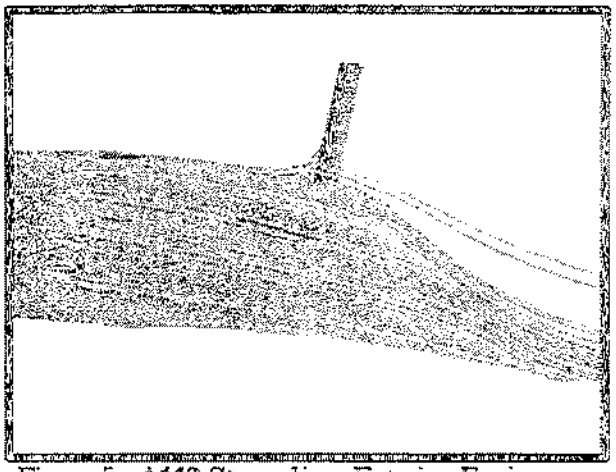

Figure 5: A119 Streamlines Entering Engine Plenum (Cruise)

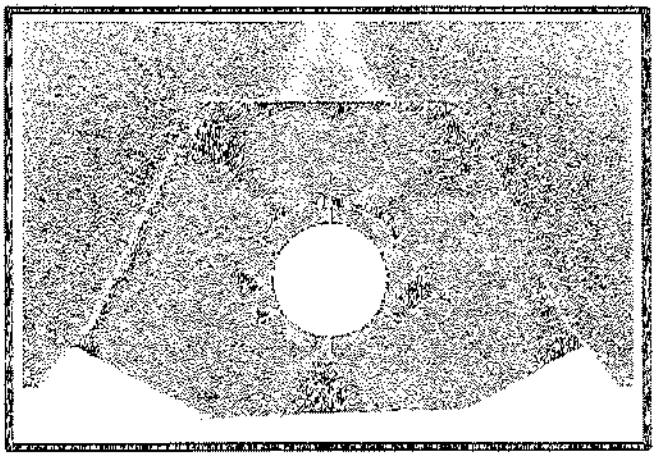

Figure 6: A119 Mach Number Distribution Inside Engine Plenum (Cruise)

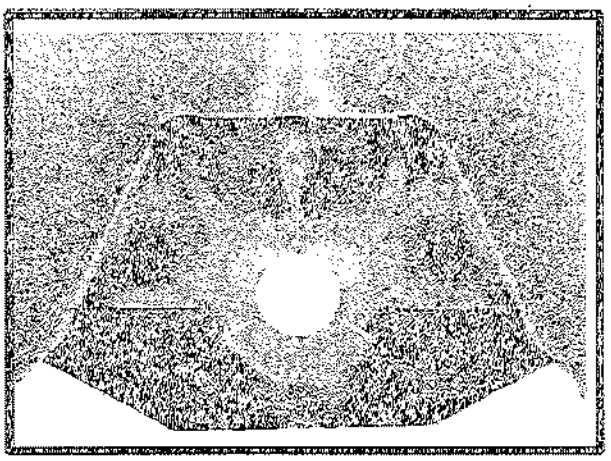

Figure 7: A119 Mach Number Distribution with Flow Divider - Axial View

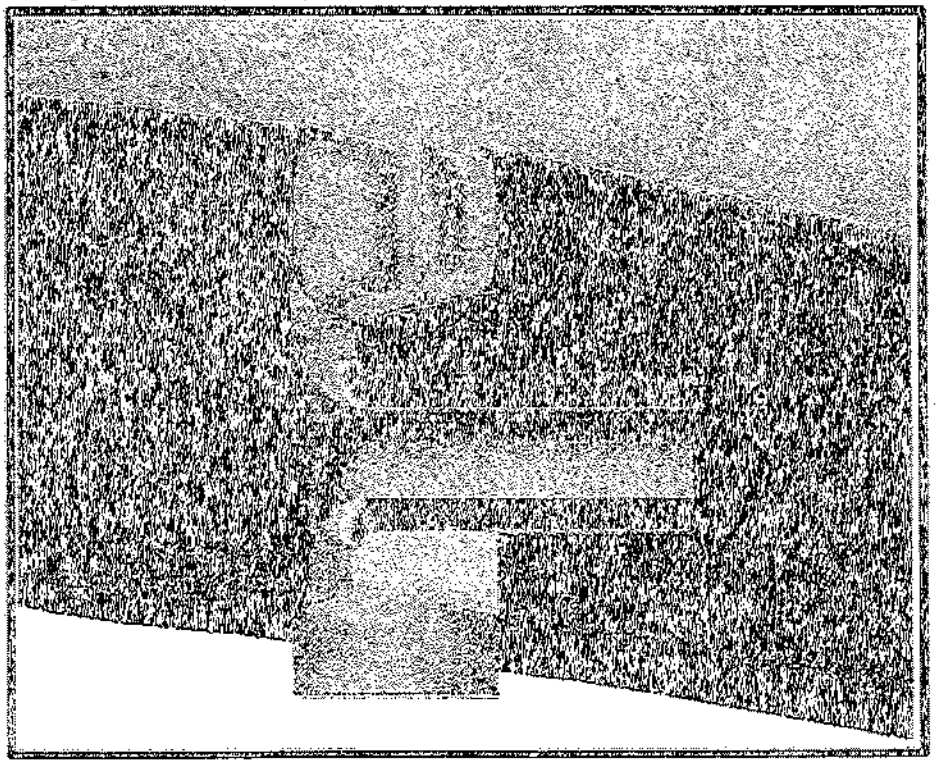

Figure 8: A119 Mach Number Distribution with Flow Divider - Side View

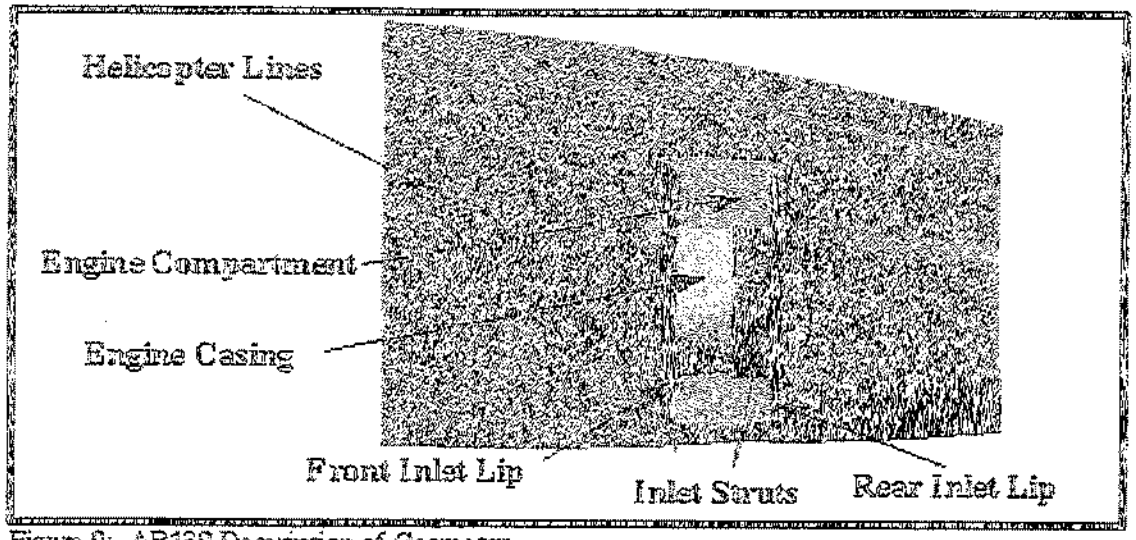

Figure 9: AB139 Description of Geometry

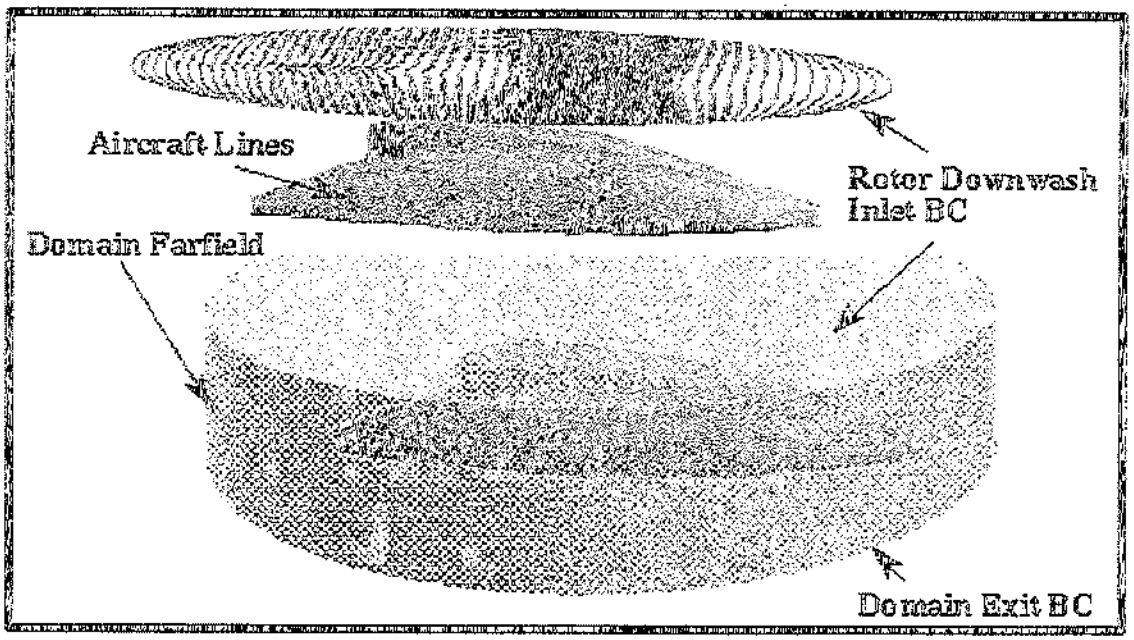

Figure 10: Computational Domain & Boundary Conditions in Hover

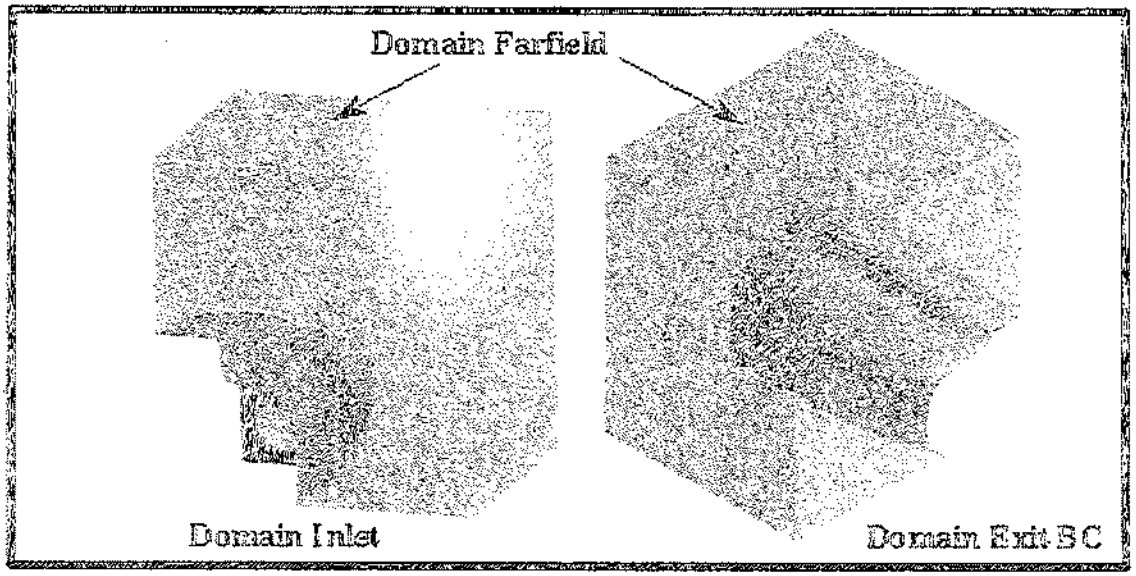

Figure 11: Computational Domain & Boundary Conditions in Forward Flight

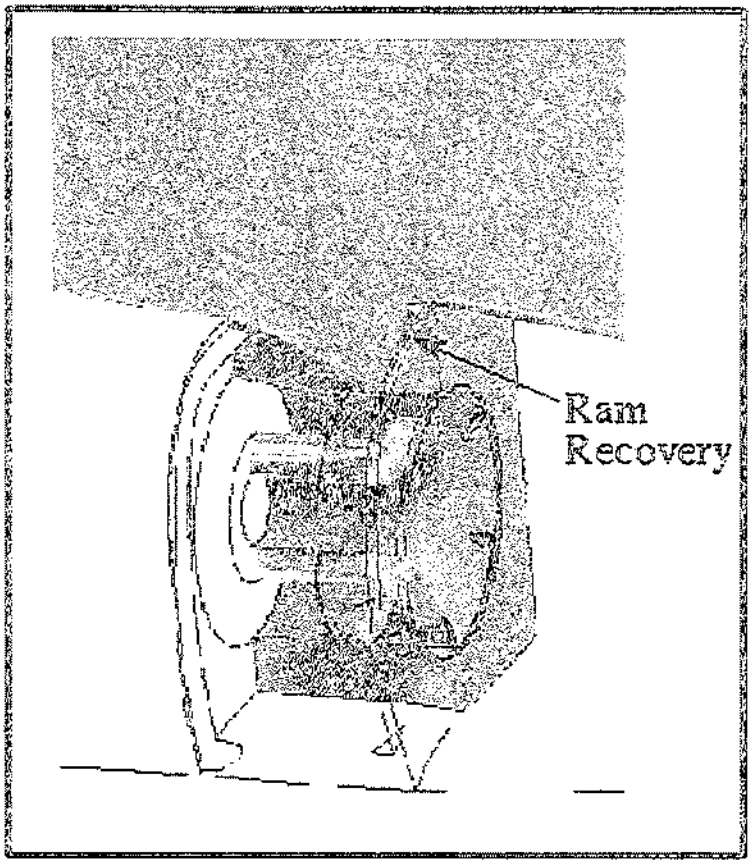

Figure 12: AB139 Ram Recovery, Mach Number Distribution

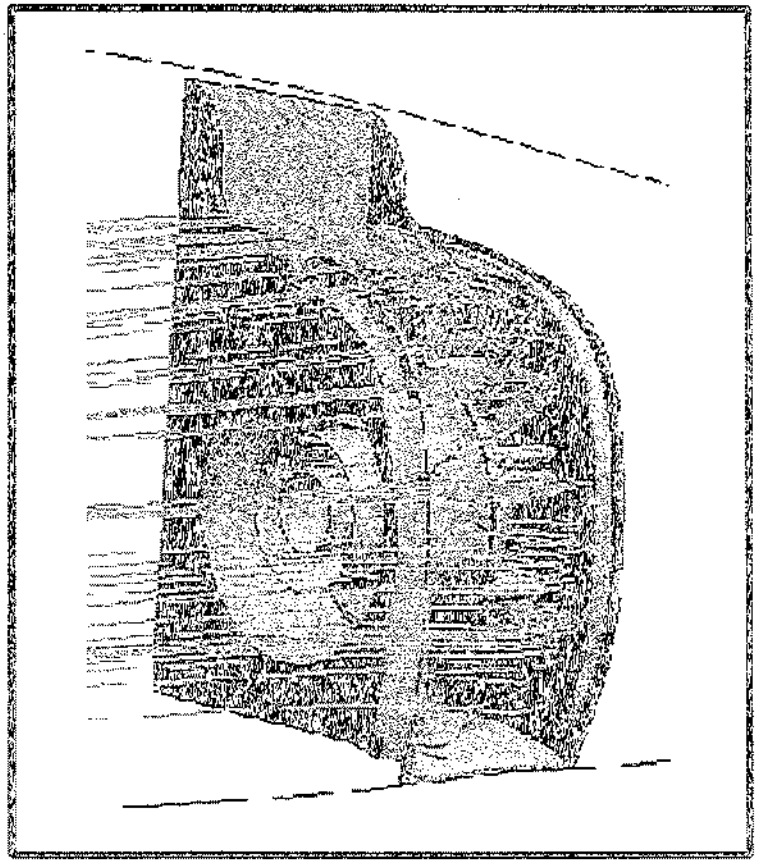

Figure 13. AB139 Streamtube, Streamlines Entering Engine Plenum

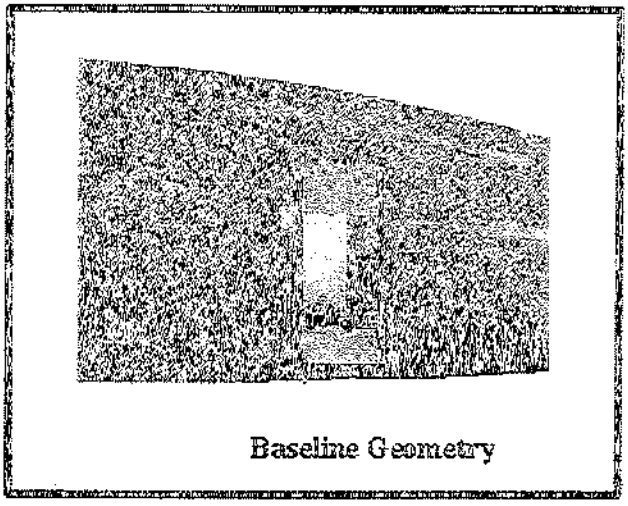

Figure 14: Geometry 1: Baseline Geometry

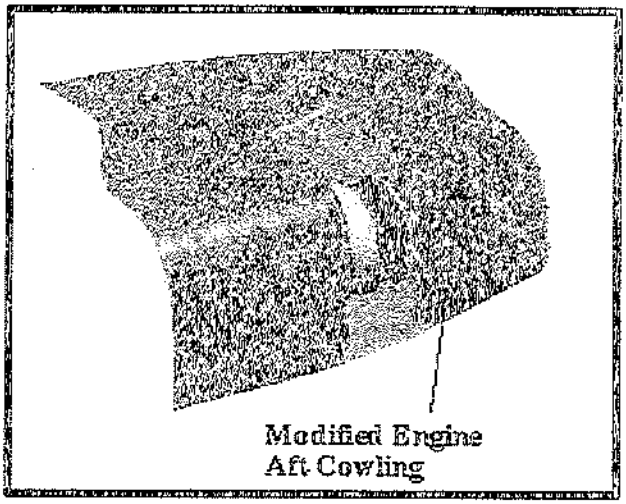

Figure 15: Geometry 2: Engine Aft Cowling Modification

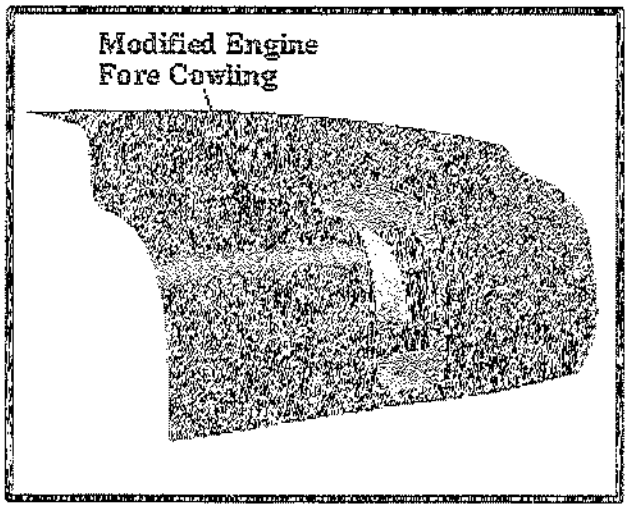

Figure 16: Geometry 3: Engine Fore Cowling Modification

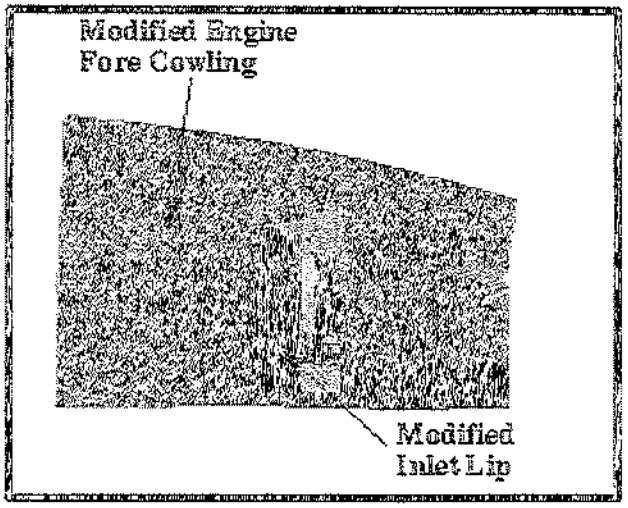

Figure 17: Geometry 4: Engine Fore Cowling & Inlet Lip Modification

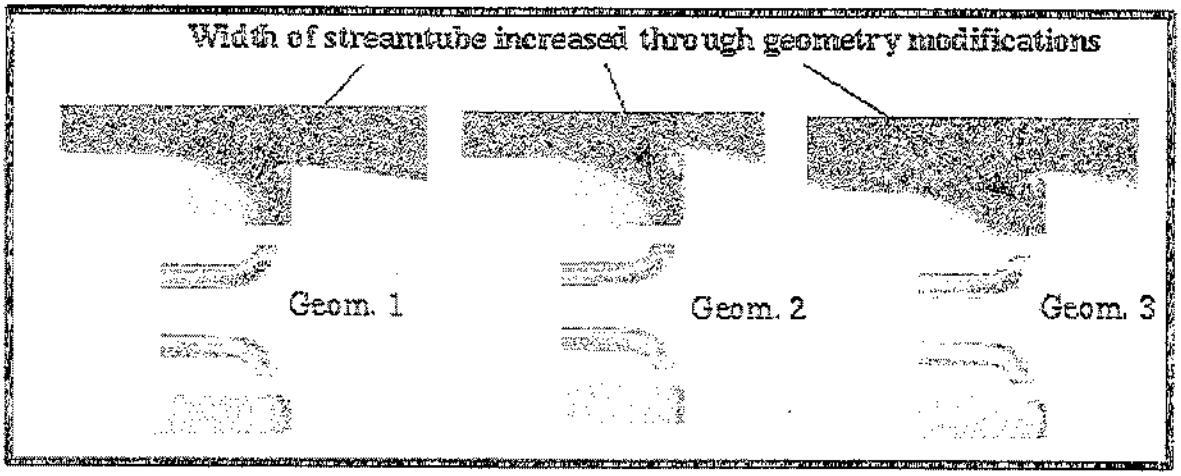

Figure 18: AB139 Total Pressure - Side View Through Engine Centerline

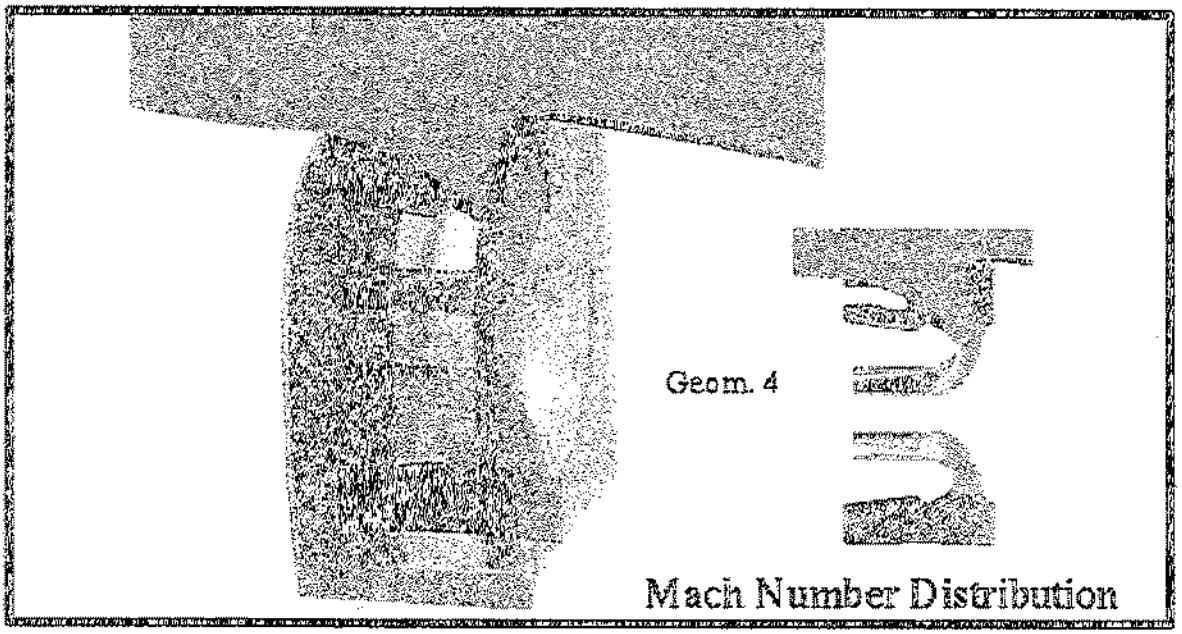

Figure 19: AB139 Inlet Lip Modification at the Upstream Side of the Engine Compartment

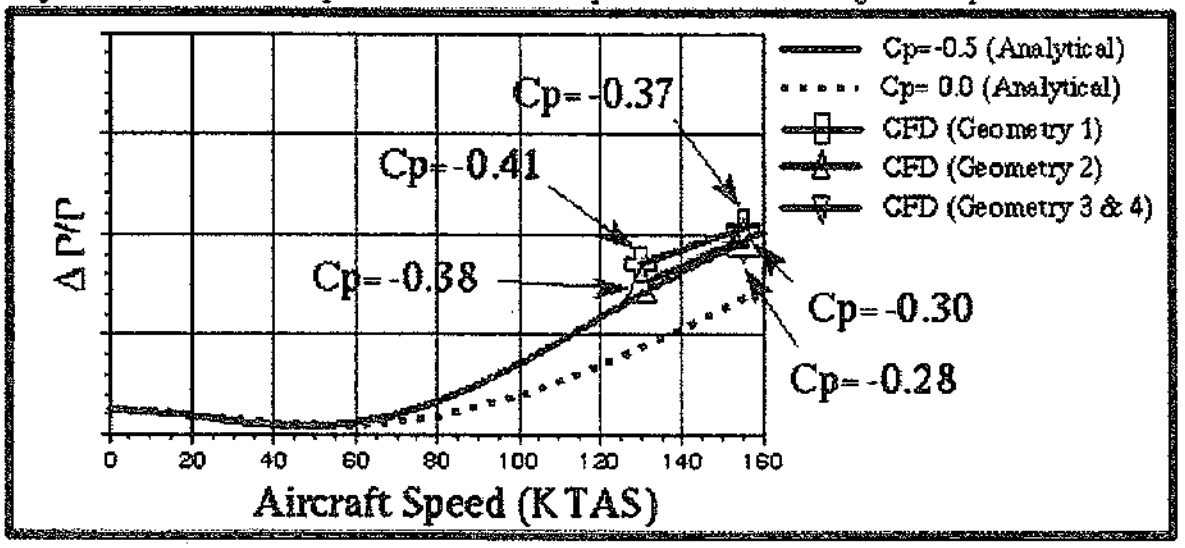

Figure 20: AB139 Inlet Pressure Losses as a Function of Aircraft Speed